

PROPAGATION AND EVOLUTION OF ICMES IN THE SOLAR WIND

John D. Richardson, Ying Liu, and John W. Belcher

*Massachusetts Institute of Technology
Cambridge, MA, USA
jdr@space.mit.edu*

Abstract

Interplanetary coronal mass ejections (ICMEs) evolve as they propagate outward from the Sun. They interact with and eventually equilibrate with the ambient solar wind. One difficulty in studying this evolution is that ICMEs have no unique set of identifying characteristics, so boundaries of the ICMEs are difficult to identify. Two characteristics present in some ICMEs but generally not present in the ambient solar wind, high helium/proton density ratios and low temperature/speed ratios, are used to identify ICMEs. We search the Helios 1 and 2, WIND, ACE, and Ulysses data for ICMEs with these characteristics and use them to study the radial evolution of ICMEs. We find that the magnetic field magnitude and density decrease faster in ICMEs than in the ambient solar wind, but the temperature decreases more slowly than in the ambient solar wind. Since we also find that ICMEs expand in radial width with distance, the protons within ICMEs must be heated. Scale sizes for He structures are smaller than for proton structures within ICMEs.

Keywords: ICME, solar wind

1. Introduction

Coronal mass ejections (CMEs) are eruptions of matter from the Sun into interplanetary space. A CME may result in the ejection of 10^{16} g of matter with a broad range of speeds, up to at least 2000 km/s [e.g., Lepping et al., 2001]. The ejected material forms an interplanetary coronal mass ejection (ICME) in the solar wind. The ICMEs that collide with Earth often produce large effects in Earth's magnetosphere; almost all of the largest geomagnetic storms result from ICMEs [Gosling, 1993].

A centerpiece of space weather research is the forecasting of ICMEs and their magnetospheric effects. Solar observations have been used to detect Earthward CMEs [i.e., Zhao and Webb, 2003]. Spacecraft monitors such as ACE and SOHO at the L1 Lagrange point provide warnings of incoming

ICMEs 30-60 minutes upstream of Earth. Proxies such as the field direction within magnetic clouds [Chen, 1996] and shocks [Jurac et al., 2002] can be used to predict geomagnetic storms. In the future, STEREO is designed to remotely sense the propagation of CMEs in the solar corona which produce Earthward-propagating ICMEs.

For long-range, several day in advance forecasting based on solar observations to succeed, we need to understand better how ICMEs evolve in the solar wind. For the shorter-term, 30-60 minute forecasting based on L1 observations, the effect of radial evolution between L1 and Earth is likely small, but since L1 monitors are often hundreds of R_E from the Earth-Sun line, we need to understand the spatial extent of CME material perpendicular to the solar wind flow. Variations in the magnetic field magnitude, plasma bulk speed, and plasma density have larger scale lengths in solar wind which causes large geomagnetic disturbances than in the typical solar wind [Jurac and Richardson, 2001], but length-scales of variations within the ICME material have not been studied.

This paper reviews the radial evolution and spatial scales of ICMEs in the solar wind. One of the difficulties in studying these subjects is that it can be difficult to identify ICMEs and their boundaries. We discuss two criteria which may be sufficient to identify ICMEs, enhanced helium abundances and lower than expected temperatures for a given solar wind speed. We use a list of ICMEs produced using these criteria which spans radial distances from 0.3 to 5.4 AU to described the radial changes in ICMEs. We also compare the helium abundances observe by ACE and WIND to determine the scale size of enhanced helium events perpendicular to the solar wind flow.

2. Identification of ICMEs

ICMEs have many identifying characteristics (see reviews by Gosling, 1990; Neugebauer and Goldstein, 1997; Gosling, 1997); among them are

- 1 The temperature is lower than normal for the observed solar wind speed.
- 2 The fluctuation level of the magnetic field magnitude is small.
- 3 The ratio of the He to H density is larger than normal but strongly fluctuating (e.g., Berdichevsky et al., 2002).
- 4 Energetic protons and cosmic rays stream along the magnetic field.
- 5 Bi-directional electrons are observed, moving in both directions along the magnetic field indicating that the field lines are closed loops connected to the Sun or to themselves.
- 6 Enhancements in minor ions such as Fe and higher charge states of heavy ions such as Fe and O (Burlaga et al., 2001; Lepri et al., 2001).

- 7 Depressed energetic particle intensities known as Forbush decreases resulting from the increased magnetic field.
- 8 Slowly rotating magnetic fields are signatures of a subset of ICMEs known as magnetic clouds.
- 9 A preceding shock formed by faster CME material encountering slower solar wind when solar counterpart observations or remote radio sensing indicate the presence of ejecta.

The problem is that, although ICMEs may have some of these characteristics, few ICMEs have all of them and many have a small subset of them. In addition, these characteristics may not persist across the entire ICME but may come and go within one ICME.

Various lists of ICMEs have been developed based on various of these criteria. We refer in this paper to the list developed by Cane and Richardson [2003] (hereafter referred to as C&R) using data from 1996 through 2002 which covered the period from solar minimum to solar maximum. The starting point for this list is the criterion that the observed temperature, T_{obs} , be less than 0.5 of the temperature expected for the observed solar wind speed, T_{exp} (Richardson and Cane, 1995). The expected temperatures for a given speed are taken from Lopez and Freeman [1986]. In addition to the temperature criterion, C&R used shocks, Forbush decreases, and energetic particle signatures (but not helium abundance or bi-directional electrons) to identify ICMEs.

Figure 1 shows 12 days of WIND data from 1999. The hatched area shows the time of an ICME from the C&R list. The ICME region lasts about two days, has a low temperature given the relatively high speed, follows a shock, and has little magnetic field variation. Although this criterion was not part of the C&R ICME search criteria, the ICME also has enhanced He abundances. This example is clearly consistent with the definition of an ICME, although some ambiguity exists as to the location of the trailing edge. But on day 260 the helium abundance also increases for about a day coincident with a small temperature decrease. Magnetic fluctuations through most of this time period are small. Based on the He abundance, this event is also likely an ICME, although the boundaries of the event are not obvious.

The hatched ICME in Figure 1 shows two other important features of ICMEs. The speed decreases across the ICME, so that the forward edge moves faster than the trailing edge. This speed difference results from expansion of the ICME. The magnetic field (and thus magnetic pressure) is high with the first half of the ICME; many ICMEs have a larger internal pressure than does the ambient solar wind, also leading to expansion of the ICME as it moves outward.

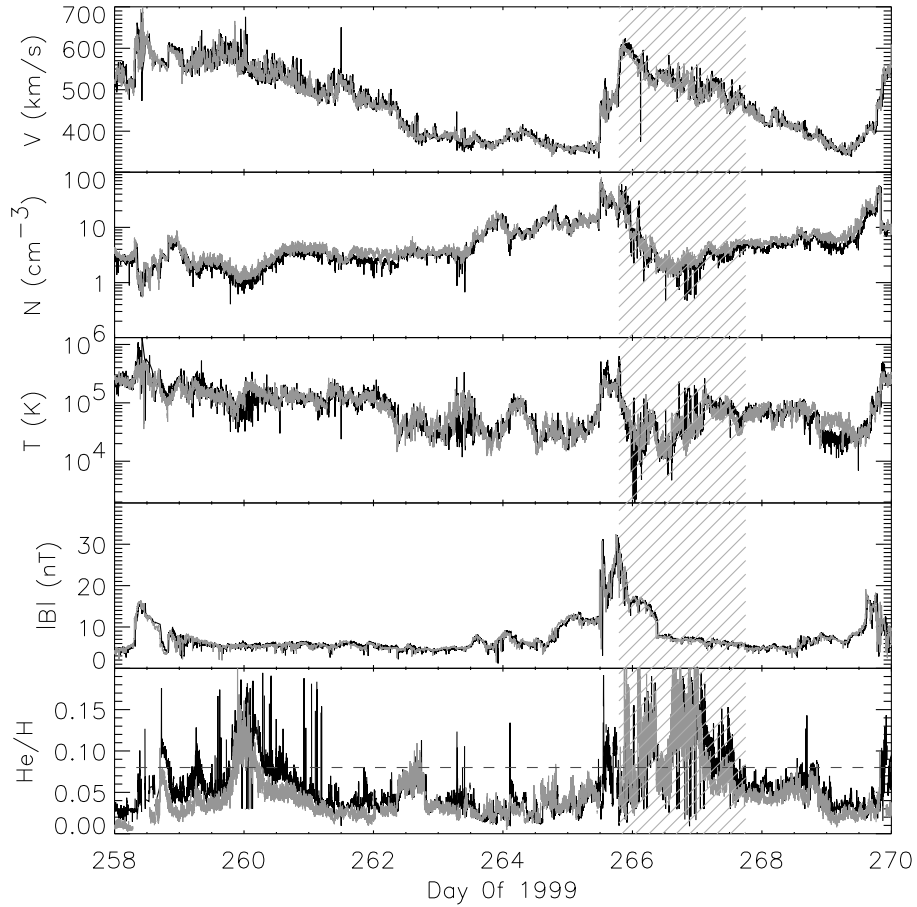


Fig. 1. Solar wind speed, density, temperature, magnetic field magnitude, and helium/proton density ratios from WIND (black) and ACE (gray). The hatched region is a ICME identified by C&R. The dashed line in the bottom panel shows the 0.08 helium to proton density ratio considered sufficient to identify ICME plasma.

The examples in Figure 1 show the difficulties inherent in the study of ICMEs; namely determining if they are present and when they start and end. In a few cases when ICMEs have apparently been larger in angular extent than the spacecraft separation, the same ICME has been observed at widely separated radial distances. For example, the Bastille day 2001 CME occurred when Earth and Voyager 2 were at nearly identical heliolongitudes and was observed at 1 AU and 63 AU [Wang et al., 2001]. But since radial alignments of spacecraft are rare, we want to look at ICME evolution on a statistical basis. We

choose two ICME characteristics that are thought to be sufficient (but not necessary) to identify ICMEs; 1) $T_{obs}/T_{exp} < 0.5$ and 2) $N_{He}/N_H > 8\%$. This method makes the implicit assumption that ICMEs with these characteristics are typical of ICME plasma.

We identify the times in the Helios 1 and 2, WIND, ACE, and Ulysses data that both these criteria are met. Helios 1 and 2 operated from 1976 to 1980 and 1976 to 1985, respectively, at distances of 0.3 to 1 AU. WIND was launched in late 1994 and is near 1 AU. ACE was launched in 1997 and orbits Earth's L1 Lagrange point. Ulysses was launched in 1990 and orbits over the solar poles at 1.3 - 5.4 AU (although most ICMEs detected are at low latitudes). Since the temperature decreases with distance, we normalized to 1 AU assuming a R^{-1} dependence [Totten et al., 1995; see also Steinitz and Eyni, 1981; Lopez and Freeman, 1995] before applying the temperature criteria. The N_{He}/N_H ratio should be independent of distance which makes it a useful tracer of ICMEs [Paularena et al., 2001]. The complete list of ICMEs we identified using these criteria is given by Liu et al. [2004].

3. Radial Evolution of ICMEs

Figure 2 shows the distribution of ICMEs at 1 AU from ACE and WIND

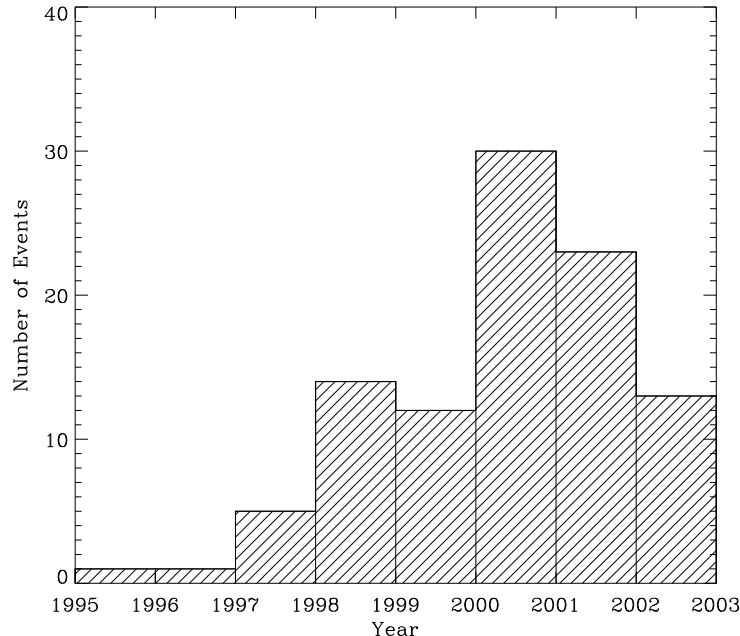


Fig. 2. Number of ICMEs at 1 AU as a function of time.

over a solar cycle using the above criteria. The solar cycle dependence is as expected, with less ICMEs at solar minimum than at solar maximum. We note that adherence to these criteria results in about 50% less ICMEs than in the C&R list. Also note that not all the magnetic clouds identified by the WIND magnetic field instrument (http://lepmfi.gsfc.nasa.gov/mfi/mag_cloud_pub1.html) are on our list, reinforcing the uncertainty inherent in choosing ICMEs.

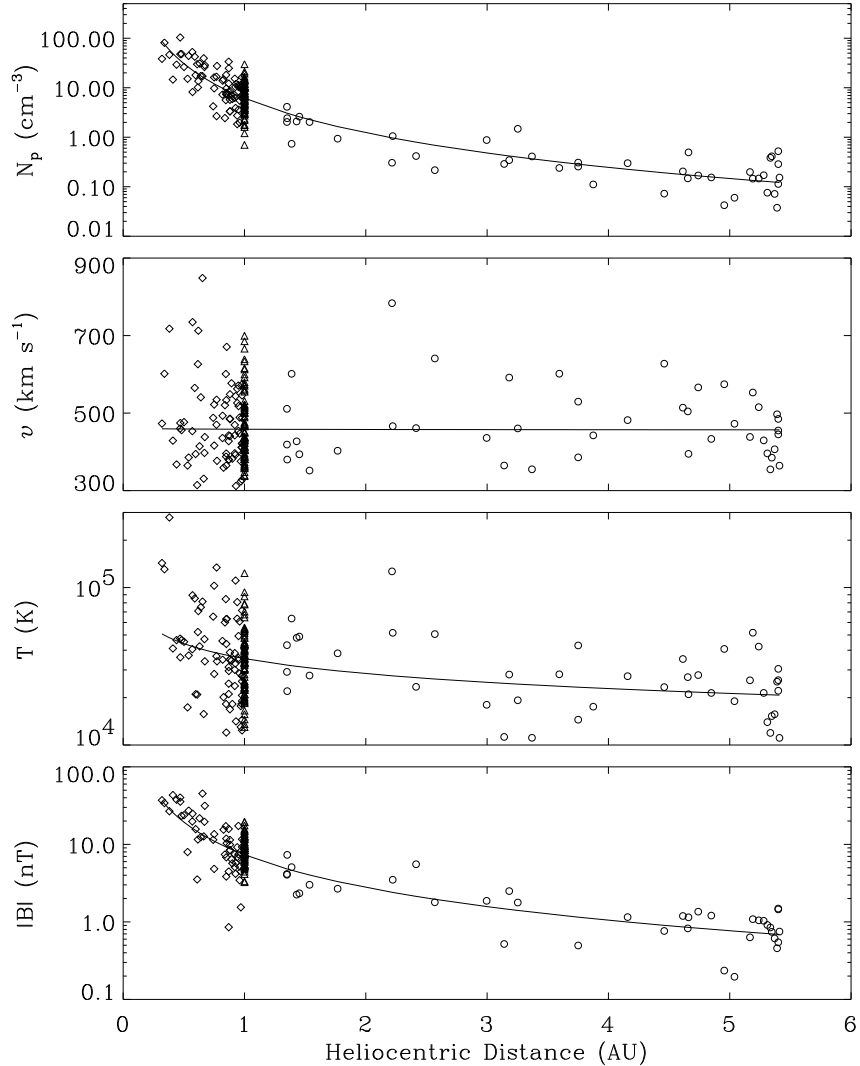


Fig. 3. Average values of the density, speed, temperature, and magnetic field magnitude within ICMEs as a function of distance. Also shown are power law fits to each parameter.

Figure 3 shows the average solar wind density, speed, temperature, and magnetic field magnitude within ICME plasma. The circles show data from Helios 1 and 2, the triangles from WIND and ACE, and the squares from Ulysses. The solid lines show the best fit of a power law to the data. The top panel shows that the density profile which best fits the data is $N(r)=6.2 R^{-2.3}$. The average density (normalized to 1 AU) in the ICMEs of 6.2 is slightly less than the 7 cm^{-3} in the background solar wind, consistent with previous results [Crooker et al., 2000]. The decrease with R is faster than in the background solar wind; as expected, the solar wind density as a whole decreases as R^{-2} out to 70 AU [Richardson et al., 2003]. The more rapid decrease of density within ICMEs is due to the expansion of the ICMEs, as discussed above.

The second panel of Figure 3 shows the average speed within the ICMEs. The fit line shows that the average speed is about 450 km/s and does not change with distance. This is comparable to the average speed of all solar wind near Earth, 440 km/s. The variations of the ICME speeds decrease with distance.

The third panel shows the temperature in ICMEs. The best fit is $T(r) = 3.5 \times 10^4 R^{-0.3} \text{ K}$. The average solar wind temperature at 1 AU is about $9.5 \times 10^4 \text{ K}$, so the ICME temperature is well below this (as expected given that one of the ICME identification criteria is low temperature). The small R dependence of T with distance was unexpected. The temperature of the background solar wind in the inner heliosphere decreases as R^{-1} [Totten et al., 1995]. Since ICMEs expand with distance, the temperature in ICMEs should decrease faster than in the background solar wind due to adiabatic cooling; instead it decreases less quickly. This result implies that significant heating of the protons in the ICMEs takes place, more than in the normal solar wind. ICMEs are often associated with streaming electrons and high heat flux; some of this energy may couple to the protons.

The bottom panel shows the magnetic field magnitude within the ICMEs. The fit to the data gives $B(r)=7.4 R^{-1.4} \text{ nT}$. For an ideal Parker spiral, the radial component of B decreases as R^{-2} and the tangential field as R^{-1} . The average magnetic field in the solar wind at 1 AU is 6.3 nT, so B is larger within ICMEs. The higher B is what results in the higher internal pressure within ICMEs which contributes to their expansion. The best power law fit to the magnetic field magnitude observations in the low-latitude background solar wind gives a $R^{-1.1}$ decrease. Thus the magnetic field within ICMEs decreases faster than that in the solar wind as a whole, again consistent with ICMEs expanding with distance.

One of the characteristics of an ICME is that the speed of the leading edge is generally greater than the speed of the trailing edge, which results in a dynamic expansion of the ICME. Figure 4 shows how Δv , the difference between the speeds on the leading and trailing edges, changes with distance. The average

value of Δv only has a small change, from about 65 to 45 km/s, but the scatter decreases quickly with distance and few ICMEs beyond 5 AU have large Δv .

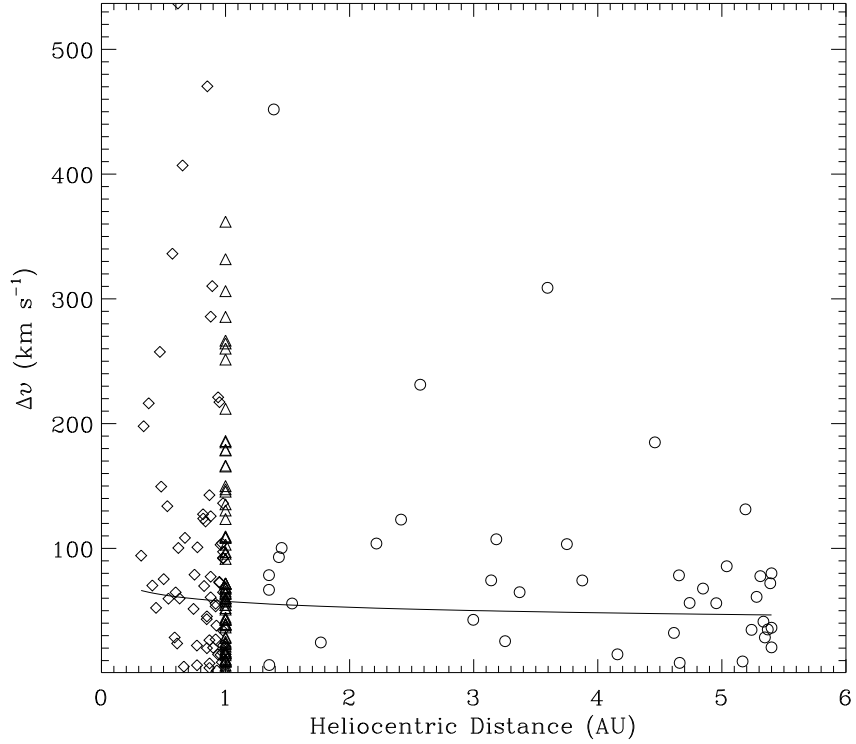


Fig. 4. The speed difference, Δv , across the ICMEs as a function of distance. Diamonds show Helios 1 and 2 data, triangles show ACE and WIND data, and circles show Ulysses data.

Figure 5 shows the radial width of ICMEs as a function of distance, where the width is determined by multiplying the time it takes an ICME to pass the spacecraft by the average speed of the ICME. The average ICME length increases from 0.25 AU at 1 AU to about 1 AU at 5 AU, a factor of four increase. Thus the expansion of ICMEs inferred from observations is a measurable, and significant, effect.

4. Spatial Scales

The space weather program resulted in numerous studies of the scale lengths of plasma and magnetic field features in the solar wind. Plasma features have scale lengths of order $100 R_E$ while magnetic field scale lengths are tens of R_E [Paularena et al., 1998; Zastenker et al., 1998; Richardson and Paularena,

2001]. Scale lengths were longer for geoeffective solar wind features [Jurac and Richardson, 2001].

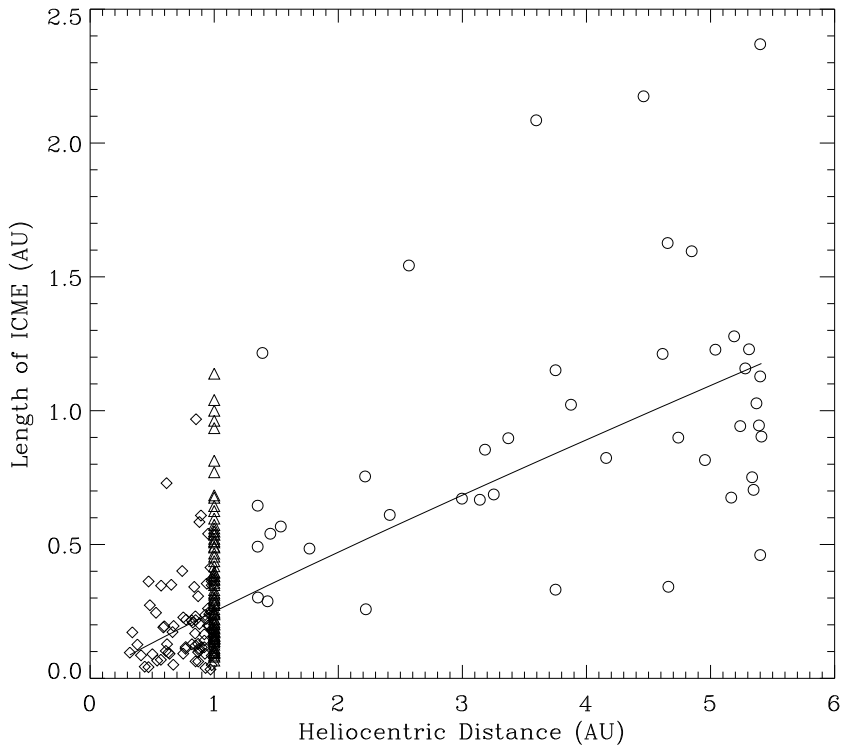


Fig. 5. The radial width of the observed ICMEs as a function of distance. Diamonds show Helios 1 and 2 data, triangles show ACE and WIND data, and circles show Ulysses data.

The regions of He enhancement are thought to be prominence material which has its origin lower on the solar surface. The He enhancements are often patchy and variable, but it has not been clear whether these are temporal or spatial variations. Since WIND and ACE provide He data near Earth, we can investigate the scale sizes of the He enhancements. As in previous work, we look at six hour segments of data from two spacecraft. The data are time-shifted using the observed solar wind speed to account for the radial separation of the spacecraft. We then perform correlations on the data as a function of lag.

Figure 6 shows correlations as a function of the He/H ratio. We did not specifically separate out ICME regions in this part of the study, but most of the high He/H regions are likely ICMEs. The top 3 panels show that the speed,

density, and B correlations are better when He/H ratios are greater than about 5%, consistent with the Jurac and Richardson [2001] results. The bottom panel shows the He/H correlations; these correlations are not significantly better for higher He/H ratios.

To determine scale lengths of the solar wind, we look at correlations as a function of spacecraft separation perpendicular to the solar wind flow. To maintain meaningful statistics, we divide the data into times when the He/H ratio is less than 4% and times it is greater than 5%.

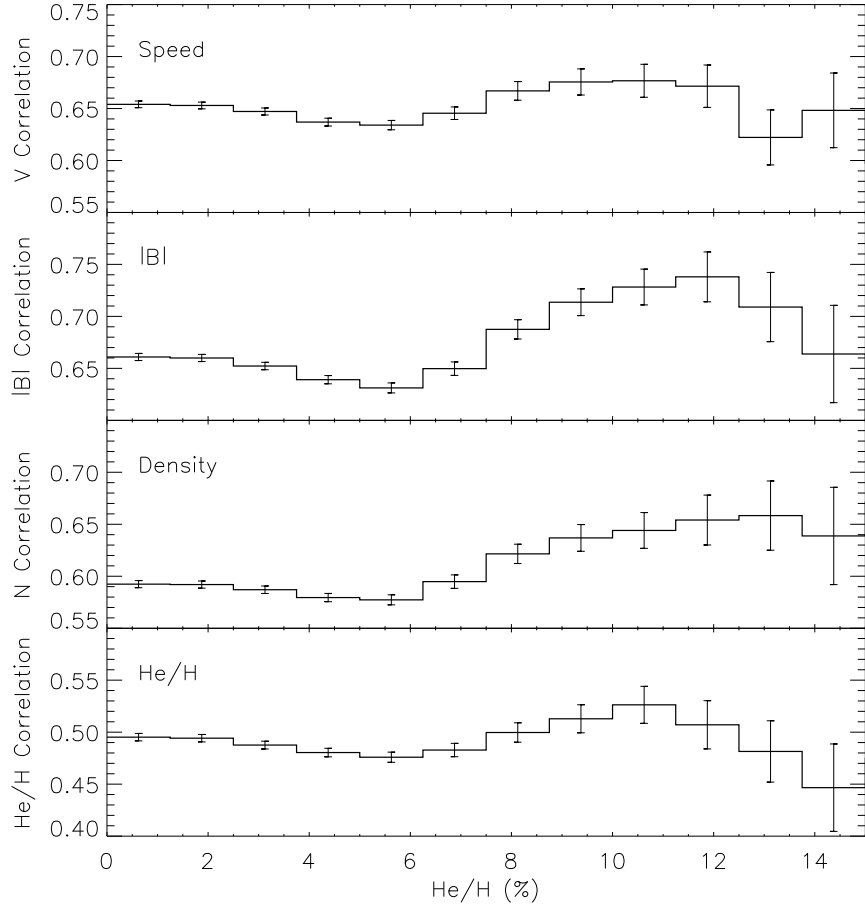


Fig. 6. Correlations as a function of the He/H ratio.

Figure 7 shows the correlations of density and He/H ratio as a function of Y_{GSE} -separation of the spacecraft for these two cases. The density correlations are fairly constant out to separations of about $220 R_E$ for the low He

case and $250 R_E$ for the large He case. For the low He case, the He/H ratio correlations are very similar to those for the density. This implies the source regions of the protons and He vary similarly. For the case where He/H is greater than 5%, which should be predominately ICME plasma, the scale length of the He/H correlations is much smaller than for the proton density, with a decrease in correlations at about $140 R_E$. Thus the He seems to be generated by a small region of a much bigger ICME source structure.

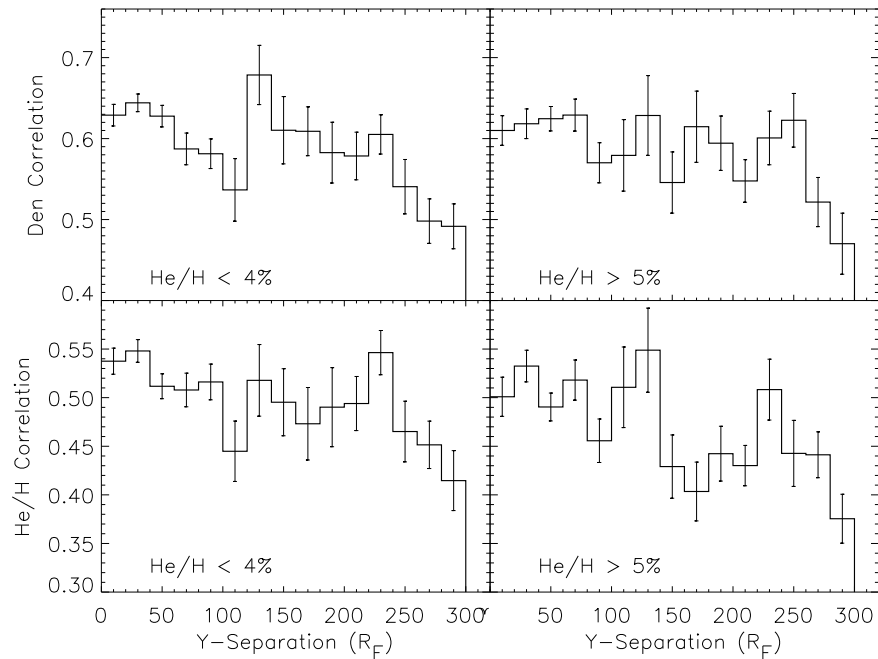


Fig. 7. Correlations as a function of the Y_{GSE} -separation of the spacecraft for $\text{He}/\text{H} < 4\%$ and $\text{He}/\text{H} > 5\%$.

5. Summary

We investigated the radial evolution and spatial scales of ICMEs. We used the temperature/speed ratio and the He/H ratio criteria to identify ICMEs in spacecraft at positions from 0.3 to 5.5 AU from the Sun. We then investigated ICME evolution in a statistical sense and find that ICMEs are about a factor of 4 larger in radial width at 1 than at 5 AU. The density and magnetic field magnitude within ICMEs decrease faster than those in the background solar

wind. These data are interpreted as indicating that ICMEs expand with distance out to at least 5 AU. The temperature decreases less fast in ICMEs than in the solar wind, opposite to expectations for a radially expanding (and thus adiabatically cooling) structure, which implies that the ICME plasma is heated significantly more than the background solar wind. The spatial scales of He perpendicular to the solar wind flow are similar to that of the density in normal solar wind, but are about half the length scales of protons in the ICMEs.

Acknowledgments

We are grateful to the ACE science center for providing the ACE plasma and magnetic field data, to the ESA Ulysses web page for the Ulysses data, to J. Kasper and A. Lazarus for the WIND alpha data, and to R. Schwenn for the Helios data. The work at MIT was supported NASA grant NAG-10915 and by NSF grants ATM-9810589, ATM-0203723 and ATM-0207775.

References

- Berdichevsky, D. B., Farrugia, C. J., Thompson, B. J., Lepping, R. P., Reames, D. V., Kaiser, M. L., Steinberg, J. T., Plunkett, S. P., and Michels, D. J. 2002, Halo-coronal mass ejections near the 23rd solar minimum: Lift-off, inner heliosphere, and in situ signatures, *Ann. Geophys.*, 20, 891, 2002.
- Burlaga, L. F., Skoug, R. M., Smith, C. W., Webb, D. F., Zurbuchen, T. H., Reinard, A., Fast ejecta during the ascending phase of solar cycle 23: ACE observations, 1998-1999 *J. Geophys. Res.*, 106, 20,957-20,978, 2001.
- Cane, H. V. and I. G. Richardson, Interplanetary coronal mass ejections in the near-Earth solar wind during 1996-2002, *J. Geophys. Res.*, 108, 10.1029/2002JA009817, 2003.
- Chen, J., Theory of prominence eruption and propagation: Interplanetary consequences, *J. Geophys. Res.*, 101, 27,499-27,519, 1996.
- Crooker, N. U., S. Shodhan, J. T. Gosling, J. Simmerer, R. P. Lepping, J. T. Steinberg, and S. W. Kahler, Density extremes in the solar wind, *Geophys. Res. Lett.*, 27, 3769-3772, 2000.
- Gosling, J.T., Coronal mass ejections and magnetic flux ropes in interplanetary space, in *Physics of Magnetic Flux Ropes*, ed. C.T. Russell, E.R. Priest, and L.C. Lee, Geophys. Mono. 58, AGU, 343, 1990.
- Gosling, J. T., Coronal mass ejections: An overview, in *Coronal Mass Ejections*, edited by N. Crooker, J. A. Joselyn, and J. Feynman, Geophysical Monograph 89, American Geophysical Union, p. 9, 1997.
- Gosling, J. T., The solar flare myth, *J. Geophys. Res.*, 98, 18937-19,949, 1993.
- Jurac, S. and J. D. Richardson, The dependence of plasma and magnetic field correlations in the solar wind on geomagnetic activity, *J. Geophys. Res.*, 106, 29,195-29,206, 2001.
- Jurac, S., J. C. Kasper, J. D. Richardson, and A. J. Lazarus, Geomagnetic disturbances and their relationship to interplanetary shock parameters, *Geophys. Res. Lett.*, 10.1029/2001GL014034, 2002.
- Lepping, R. P., Berdichevsky, D. B., Burlaga, L. F., Lazarus, A. J., Kasper, J., Desch, M. D., Wu, C.-C., Reames, D. V., Singer, H. J., Smith, C. W., Ackerson, K. L., The Bastille day magnetic clouds and upstream Shocks: Near-earth interplanetary observations, *Solar Phys.* 204, 285-303, 2001.

- Lepri, S. T., Zurbuchen, T. H., Fisk, L. A., Richardson, I. G., Cane, H. V., Gloeckler, G., Iron charge distribution as an identifier of interplanetary coronal mass ejections *J. Geophys. Res.*, 106, 29,231-29,238, 2001.
- Liu, Y., J. D. Richardson, and J. W. Belcher, A Statistical Study of the Properties of Interplanetary Coronal Mass Ejections from 0.3 to 5.4 AU, *Plan. Sp. Sci.*, in press, 2004.
- Lopez, R. E., and J. W. Freeman, Solar wind proton temperature-velocity relationship *J. Geophys. Res.*, 91, 1701-1705, 1986.
- Neugebauer, M. and R. Goldstein, Particle and field signatures of coronal mass ejections in the solar wind, in *Coronal Mass Ejections*, edited by N. Crooker, J. A. Joselyn, and J. Feynman, AGU, Washington, pp. 245, 1997.
- Paularena, K. I., G. N. Zastenker, A. J. Lazarus, and P. A. Dalin, Solar wind plasma correlations between IMP 8, INTERBALL-1 and WIND, *J. Geophys. Res.*, 103, 14,601-14,617, 1998.
- Paularena, K. I., C. Wang, R. von Steiger, and B. Heber, An ICME observed by Voyager 2 at 58 AU and by Ulysses at 5 AU, *Geophys. Res. Lett.*, 28, 2755-2758, 2001.
- Richardson I.G., Cane, H.V, 1995. Regions of abnormally low proton temperature in the solar wind (1965-1991) and their association with ejecta, *J. Geophys. Res.*, 100, 23397.
- Richardson, J. D. and K. I. Paularena, Plasma and magnetic field correlations in the solar wind, *J. Geophys. Res.*, 106, 239-251, 2001.
- Richardson, J. D., C. Wang, and L. F. Burlaga, The solar wind in the outer heliosphere, *Adv. Sp. Res.*, in press, 2003.
- Steinitz, R. and M Eyni, Competing effects determining the proton temperature gradient in the solar wind, in *Solar Wind Four*, edited by H. Rosenbauer, MPI Katlenburg-Lindau and MPI Garching, MPAE-W-100-81-31, pp. 164-167, 1981.
- Totten, T. L., Freeman, J. W., Arya, S., An empirical determination of the polytropic index for the free-streaming solar wind using Helios 1 data, *J. Geophys. Res.*, 100, 13-18, 1995.
- Wang, C., J. D. Richardson, and L. Burlaga, Propagation of the Bastille Day 2000 CME shock in the outer heliosphere, *Solar Phys.*, 204, 413-423, 2001.
- Zastenker, G. N., P. A. Dalin, A. J. Lazarus, and K. I. Paularena, Comparison of solar wind parameters measured simultaneously by several spacecraft (in Russian), *Kosm. Issled.*, 36, 228-240, 1998. (*Cosmic Res.*, 36, 214-225, 1998.)
- Zhao, X. P., and D. F. Webb, Source regions and storm effectiveness of frontside full halo coronal mass ejections, *J. Geophys. Res.*, 108, 10.1029/2002JA009606, 2003.